Quantum Electronics **32** (12) 1085 – 1098 (2002) ©2002 Kvantovaya Elektronika and Turpion Ltd

PACS numbers: 42.55.Px; 42.60.Lh
DOI: 10.1070/QE2002v032n12ABEH002351

Semiconductor lasers: from homojunctions to quantum dots

P.G. Eliseev

***Abstract*. A brief review of the development of physics and technology of semiconductor lasers, beginning from theoretical proposals made in the late 1950s up to now, is presented. For example, the threshold current density at room temperature, which was $10^5 - 10^6$ A cm^{-2} in 1963, has been now reduced to ~ 10 A cm^{-2}. The main factors that have provided this progress are considered. The mechanisms of energy conversion determining the high efficiency of semiconductor lasers are discussed in detail.**

Keywords: *homolasers, heterolasers, quantum well lasers.*

1. Introduction

A semiconductor diode laser is the most compact, economical, and reliable laser among the entire variety of lasers. Without any exaggeration, this laser has virtually become a 'laser-in-each-home'. Miniature laser crystals, based mainly on GaAs and relative materials, are used in CD and DVD players, laser printers and computers. When we phone somebody, we are usually 'served by' communication semiconductor lasers based on InP and related materials. Diode lasers are irreplaceable in modern industrial, home, and scientific devices. Millions of them are being produced monthly, and their production is constantly growing. Telephones and various types of cable communications have also acquired the second breath due to the use of semiconductor lasers.

The applications of laser diodes in various devices proved to be so natural that it seems now that they have always existed. However, their history spans only slightly more than 40 years – the first laser diodes were created in 1962. In 1959, even in pre-laser times, N.G. Basov, B.M. Vul, and Yu.M. Popov showed how to make from a semiconductor a quantum-mechanical generator and an amplifier, i.e., a source of coherent electromagnetic radiation (which is called now a laser) [1]. They proposed to use a reversible electron discharge (breakdown) for achieving excess carriers at high concentrations. The electric discharge was then successfully used in gas lasers, while breakdown-pumped semiconductor lasers were created somewhat later.

Academician Nikolai Gennadievich Basov was an enthusiast of the creation and development of semiconductor lasers. In 1961, he (together with O.N. Krokhin and Yu.M. Popov [2]) proposed to use the p – n junction in a degenerate semiconductor to obtain, as they said then, a state with a negative temperature, i.e., with the population inversion required for the operation of a semiconductor laser [2]. They derived the expression describing such a state, which remains valid up to now. They also pointed out that the interface between the regions in a semiconductor with different concentrations of carriers reflects electromagnetic waves [2] and, therefore, can be used to form the modes of an optical resonator.

These ideas were soon realised experimentally by several research groups [3 – 8]. The first diode lasers on p – n junctions (homostructures) in GaAs were created, which emitted coherent light at 850 nm [3, 4, 6 – 8], as well as variants of these lasers (GaAsP) emitting red light [5]. Somewhat earlier, a required state with the negative temperature was probably already achieved when high-current pulses were passed through degenerate p – n junctions in GaAs [9]. The appearance of stimulated emission was manifested in a narrowing of the emission spectrum, although the power of pump pulses was insufficient for lasing. Interesting comments on the earlier stages of the development of semiconductor lasers can be found in papers [10 – 14].

Diode lasers have undergone many developmental and refinement stages for 40 years and have become the most popular modern lasers. Here, we mention the creation of a variety of semiconductor lasers covering a broad spectral range (from UV to IR), the improvement of the quality of laser materials (crystals without dislocations), and the development of single-mode laser structures. A great progress has been achieved in the semiconductor technology, which allows one to control the growth of monolayers and, for example, quantum dots – atom-like objects with a volume as small as $\sim 10^{-18}$ cm^3.

The parameters of laser diodes have been improved at three main stages of their development in passing to: (i) epitaxial methods for manufacturing diode structures; (ii) heterostructures [15 – 17]; and (iii) reduced-dimension structures such as quantum wells, wires, and dots. This resulted in the reduction of the threshold current density of diode lasers at room temperature by a factor of $10^4 - 10^5$. Another very important property of a diode laser, its service

P.G. Eliseev P.N. Lebedev Physics Institute, Russian Academy of Sciences, Leninskii prosp. 53, 119991 Moscow, Russia;
Present address: Center for High-Technology Materials, University of New Mexico, Albuquerque, USA; e-mail: eliseev@chtm.unm.edu

Received 20 September 2002
Kvantovaya Elektronika **32** (12) 1085 – 1098 (2002)
Translated by M.N. Sapozhnikov

life, was increased from only several seconds for the first cw lasers to millions of hours for modern lasers.

N.G. Basov not only foresaw a brilliant future of semiconductor lasers but also spent great efforts to develop this scientific field. He became aware of the potential advantages of semiconductor lasers before others, and especially emphasised the possibility of highly efficient energy conversion in these lasers (at the time when their real emission efficiency was very low); their fast response, which could provide the application of semiconductor lasers in broadband optical communication systems and in ultrafast computers, which he considered no less important; as well as their compactness and the possibility of their compatibility with integrated circuits.

As for practical applications of semiconductor lasers, N.G. Basov came to the conclusion as early as 1970s that semiconductor lasers should be used in facilities for laser thermonuclear fusion at the intermediate stage of energy conversion, namely, for optical pumping. Thermonuclear fusion remains a main hope for solving the energy problem of the mankind in the future. However, the efficiency of the first laser facilities capable of initiating a thermonuclear reaction was so low that the total energy balance was unacceptable. Semiconductor lasers, which had a record efficiency of 40 % already at those times, could improve the situation. At the same time, diode lasers had low output powers and were comparatively costly.

It seemed impossible that the project proposed by N.G. Basov could be realised. Indeed, the number of semiconductor lasers contained in one laser unit intended for thermonuclear fusion should be of the order of 10^{12}!, whereas their world's production did not exceed 10^6 at that time. In addition, because the cost of one laser was about \$100, no budget could support such studies. When I told N.G. Basov about my doubts, he agreed that this project is expensive, but first the problem of manufacturing of laser diodes in great amounts should be solved. These expenditures will be compensated in future thermonuclear power plants. In addition, there are many intermediate problems whose solutions will bring economical effects, for example, laser technology.

The time has shown that there is no way to achieve laser thermonuclear fusion except using semiconductor lasers. Diode pumping proved to be indispensable in most modern industrial laser devices and units. Diode arrays containing millions of laser diodes (which are partially monolithically integrated) are now commercially available, and they are ordered mainly by researchers working in the field of laser thermonuclear fusion.

2. Basic types of semiconductor lasers

Injection-pumped lasers on interband transitions (injection lasers) occupy a prominent place in a large family of semiconductor lasers. There are different types of these lasers, in particular, vertical-cavity surface-emitting lasers (VCSELs) in which a laser beam is generated along the normal to an active layer. These lasers have already found many applications, in particular, for broadband data transmission over comparatively short distances (in practice, this is more than half the commercial market of laser communication systems). VCSELs can be readily assembled to form 1D or 2D monolithic arrays and can be used in the future in laser pumping systems. Interband transition (bipolar) lasers also include semiconductor lasers pumped in different ways: by a beam of fast electrons [18] or other fast particles, optically pumped lasers [19], electric-breakdown-pumped lasers [20], etc.

In the so-called streamer lasers, an incomplete discharge with a running streamer is used. Together with a streamer, an active region of the laser is running in the crystal, where the population inversion is produced directly behind the streamer [20]. The possibility of lasing in the longitudinal geometry upon contactless pumping, i.e., for lasers with a vertical cavity similar to that used in VCSELs, was demonstrated already in 1960s [21]. Because of a high optical gain in semiconductors in the case of longitudinal geometry, the length of the active region along the cavity axis is comparatively small, whereas the area of the emitting surface can be sufficiently large to provide a high output power ($10^5 - 10^6$ W per pulse). These lasers were called emitting-mirror lasers [21].

Along with this, the so-called unipolar semiconductor lasers on intraband transitions were created. In particular, they include hot-hole lasers [22] and quantum-cascade lasers (QCLs) [23]. The latter use transitions between subbands or discrete levels in quantum well structures, including superlattices. The pumping of the laser levels (filling of the upper level and depletion of the lower level) is produced by tunnelling, in particular, resonance tunnelling between adjacent quantum wells. There exist two unipolar radiative mechanisms: vertical transitions between the excited and ground states in a quantum well (or between different excited states) and diagonal transitions between the quantisation levels in adjacent quantum wells. A somewhat lower transition probability in the diagonal mechanism (because of an incomplete overlap of the wave functions) is compensated since unipolar heterostructures can be readily assembled monolithically (can be 'cascaded', giving the term cascade lasers). In other words, a packet of unipolar structures can be easily placed in a mode volume of the laser to produce a total gain when the gain of an individual structure is insufficient. It seems that cascade lasers will replace in the future the bipolar lasers in the IR region (3.5 – 19 μm), where the latter can operate only at low temperatures. Cascade lasers operating at 300 K in the spectral range from 5.0 to 8.4 μm were created [24], which possess parameters suitable for applications in high-resolution spectroscopy and spectral sensors [25].

3. Materials for semiconductor lasers

The most popular types of semiconductor lasers are based on the $A^{III}B^{V}$ compounds, mainly using the GaAs technology. Lasers based on the InP technology occupy the second place. In the visible range, along with InAlGaP red lasers (on a GaAs substrate), there exists a new family of laser diodes based on the GaN technology (violet lasers have been commercially available since 1999). Laboratory nitride lasers emitting UV and blue light were also developed [26 – 29], as well as lasers based on the heterostructures of solid solutions of the $A^{II}B^{VI}$ compounds (ZnSe and related compositions [30 – 32]) emitting in the blue – green region. They were also grown on GaAs substrates.

Another group of semiconductor lasers based on the $A^{IV}B^{VI}$ compounds covers a broad spectral range from 3 to 50 μm. The parameters of these lasers were significantly improved (in particular, their operating temperature was

increased). However, the application and production of these lasers is restricted by the necessity of using cryogenic equipment. Stimulated emission of polymer semiconductor diodes was reported in [33].

Because direct-gap transitions are not important in unipolar materials, such materials as Si and Ge can be used. In hot-hole lasers, nondirect gap p-Ge is predominantly used (emitting between 70 and 350 μm). In addition, there are other promising groups of laser semiconductors, which are not commercially available so far. Thus, multilayer quantum well structures based on the GaAs and InP technologies (emitting between in the range from 5 to 18 μm) are used in cascade lasers of the mid-IR range. The review of laser materials for long-wavelength lasers is presented in [34].

4. Applications of semiconductor lasers

Let us outline briefly technical applications of semiconductor lasers:

(1) CD systems for data recording and reading (CD, DVD and mini-disc players, CD drivers in computers, computer memories).

(2) Laser printers.

(3) Communication systems: long-range telephone cable communication, broadband cable communication between computers and in local networks, directional optical communication in the atmosphere and outer space, various types of signalisation.

(4) Industrial and transport automatics and robotics, 'robot vision' and various interference and pulsed sensors, rangefinders, control of precision movement in electronic industry.

(5) Readout of bar codes and instruments readings, optical pointers, 'optical guards'.

(6) Optical pumping, laser diode pumping of solid-state lasers, in particular, in laser fusion experiments.

(7) Stroboscopic illumination, active night vision, tracking, target pointing, illumination, projection imaging.

(8) High-resolution spectroscopy, especially IR molecular spectroscopy, spectroscopic sensors of impurities and hazardous gases.

(9) Laser technology: marking, microwelding and microcutting.

(10) Laser medicine: ophthalmology, surgery, anaesthesia, wound healing, 'low-dose' therapy, etc.

5. Technological evolution

Homostructures. In the period from 1962 to 1968, laser diodes of only type were known, the so-called homostructures or simply p–n junction lasers. While in 1962 only diffusion homostructures were available in laboratories, in 1963–1964 the liquid-phase epitaxy (LPE) is coming into use. This technology has an important advantage of controlling the doping profile with a greater accuracy than in the case of diffusion method. Indeed, the diffusion homostructure assumed the use of a preliminary heavily doped substrate (usually of the n-type) followed by the conversion of one type of conduction to another upon diffusion to the upper layer of the substrate. As an acceptor impurity in GaAs, zinc was used, which exhibits anomalous diffusion and provides a very high surface concentration of acceptors. Therefore, an active medium was formed in the substrate near the p–n junction, where both impurities were present, donors and acceptors, the p-type conduction being produced in this region due to recompensation. By using LPE, properly doped epilayers could be grown, which could contain uncompensated impurities, and the active region could be placed in the epilayer, which is usually more perfect than a substrate. Epitaxial structures made it possible to make the first step in the improvement of the lasing threshold. The minimum threshold current density at room temperature was reduced down to 20 kA cm^{-2} [35].

Homostructures were manufactured from a number of $A^{III}B^{V}$ compounds and covered the spectral range from 640 nm to 1.1 μm [36, 37]. Another group of homostructures was fabricated from the $A^{IV}B^{VI}$ compounds and alloys [38, 39] emitting in the mid-IR range. It is important that these spectral regions (and later a more broad range from 370 nm to 50 μm) could be covered continuously in principle by using different semiconductors and tuning the emission wavelength by varying temperature, pressure, or magnetic field.

Heterostructures. It is difficult to overestimate a drastic improvement in laser parameters that was achieved due to the use of heterostructures. Although the advantages of using a contact between two semiconductors of different types in lasers were mentioned already in the early 1960s [2, 15, 16], great efforts and technological progress were required to prove this experimentally.

The stacking of different single-crystal materials together became a new problem of epitaxial technology because the mismatch of their crystalline lattices immediately resulted in the appearance of many defects at their heterointerface, and first of all a misfit dislocation network. Such defects were inadmissible because they caused substantial losses of the pump current due to nonradiative recombination and leakage. Later, it was also found that dislocations in the active region or its vicinity are extremely undesirable because they serve as sites of an accelerated degradation. Thus, it was necessary to achieve a high structural quality of heterojunctions. The formation of misfit defects can be avoided in two ways: (i) to select materials for heterostructures with identical lattice parameters and (ii) use thin epilayers in the presence of a moderate mismatch (the critical thickness is inversely proportional to the mismatch of lattice periods).

At the beginning the first method was efficiently used. The close lattice parameters of GaAs and AlGaAs proved to be a favourable circumstance. Zh.I. Alferov *et al.* [17] demonstrated lasing in the structure with GaAs/AlGaAs heterojunctions. Later, the laser design and technology were improved. Single n-GaAs/p-GaAs/p-AlGaAs heterostructures (SHSs), in which a high-energy-gap AlGaAs semiconductor was used to form a barrier confining the diffusion of electrons into the p-region, attracted the attention of researchers for some time [40–42]. However, the asymmetry in the distribution of the dielectric constant of single structures prevented the decrease in the active-layer thickness and the reduction in the threshold current density below ~ 8 kA cm^{-2} [42]. Two-sided (double) heterostructures (DHs) proved to be more efficient [43, 44]. The reducing of the threshold current density below ~ 1 kA cm^{-2} provided cw lasing at room temperature [44–47]. This opened up tremendous prospects for practical applications and was a turning point in the production of semiconductor lasers.

The problem of reliability of laser diodes was mainly solved in 1970s (at least for low-power lasers), and a variety of laser structures were developed. In addition, more promising epitaxial technologies for heterostructure growing appeared (molecular beam and MOCVD). Beginning in 1980s, quantum well structures and corresponding technologies were rapidly developed (see Section 7).

6. Methods for confining electrons and photons used in semiconductor lasers

Heterojunctions made it possible to produce gradients or jumps of the important parameters of a semiconductor structure such as the energy gap, the position of the edges of the valence band and the conduction band, and the refractive index. The energy barriers used for the confinement of carriers within a given volume provide the electron confinement (the confinement of the drift-diffusion of carriers). The gradients or jumps of the refractive index can strongly affect the formation of a mode volume. The optical confinement of photons in laser structures is equivalent to the waveguide effect if the latter includes not only the refractive-index-guiding but also the gain-guiding. In AlGaAs/GaAs heterostructures and in other laser structures, a rule is valid according to which a material of the heterostructure with a broader energy gap has a lower refractive index (a rare exception is, for example, GaSb/InAs). Therefore, if an active low-energy-gap material placed between higher-energy-gap materials forms a potential well for excess carriers and has a higher refractive index, it proves to be simultaneously the core of an optical waveguide preventing the diffraction of laser radiation to passive regions.

Double AlGaAs/GaAs/AlGaAs [43] and InP/InGaAsP/InP [48] heterostructures are examples of good matching between the active and mode volumes. The optical confinement factor Γ for heterostructures was calculated for the first time in paper [49]. It was shown in experimental paper [50] that a strong optical confinement did occur in AlGaAs/GaAs heterostructures and the transverse size of the laser beam could be reduced in fact down to half the wavelength (as confirmed by the diffraction-limited divergence of the laser beam outside the laser). The optimisation of the heterostructure for obtaining the minimum threshold current density showed that the thickness of the active region should be reduced down to its technological limit, which is accompanied by a strong decrease in the optical confinement factor and, hence, in the mode gain [51]. However, due to a high optical gain inherent in semiconductors (which is unique among all the lasers), one can expect a decrease in the lasing threshold with decreasing the active-layer thickness d.

Separate-confinement heterostructures (SCHs), where the active and mode volumes are optimised independently, offer the most wide possibilities [52–54]. Such heterostructures are also most popular now, when the active region in most laser structures consists of one or several quantum wells placed inside an optical waveguide, which in turn is located between high-energy-gap cladding layers (emitters in the Russian literature). Heterostructures with an ultrathin active layer, in which quantum-size effects are observed, are called quantum wells. Note that among heterostructures with an ultrathin active layer, SCHs have the greatest optical confinement factor. It was shown that the factor $\Gamma \sim d^2$ in DHs, whereas $\Gamma \sim d$ in SCHs [55]. As a result, the mode optical gain in quantum well SCHs is an order of magnitude higher than that in quantum well DHs when the material gain in these structures is the same, i.e., for the same pump density.

7. Lasers based on reduced-dimension structures

In the early 1980s, quantum well lasers attracted the attention of researchers. Note that the term quantum wells refers historically to the structures that are confined over one coordinate (i.e., to a two-dimensional electron-hole gas). Structures with a two-dimensional confinement and one translational degree of freedom are called quantum wires, and structures with a three-dimensional restriction are called quantum dots. The quantisation levels in ultrathin AlGaAs structures were observed as early as 1974 [56].

The threshold current density in semiconductor lasers was reduced due to several factors. On the one hand, these were purely technological advances (the use of precision technologies of epitaxial growth accompanied by the control of a monolayer thickness, the use of quantum wires and quantum dots, etc.) and on the other hand, the active volume was reduced and quantum-size effects were used.

The active-medium-volume factor. In the first generation lasers (homolasers), the active-medium volume could not be controlled reliably because injected carriers could freely migrate inside a semiconductor. The active volume depended in fact on the penetration depth of carriers. For example, if migration of electrons is described by the diffusion length L, then the distribution of the concentration of excess electrons is $N_e(x) = N_{e0} \exp(-x/L)$, where N_{e0} is the concentration at the p–n junction. If the population inversion is achieved at the lasing frequency when the electron concentration is N^*, then the thickness of a region where the inversion takes place (in the p-region, where $N^* < N_{e0}$) will be $d = L \ln(N_{e0}/N^*)$. The value of d can differ from the diffusion length L and, in addition, it proves to be variable because N^* depends on the lasing frequency. A similar situation is also observed upon nonlinear recombination, when the electron distribution has a more complicated profile.

These factors were ignored in earlier calculations and the active-region thickness was assumed to be of the order of L. Note that the active region in some epitaxial homostructures was intentionally made as a strongly compensated semiconductor, thereby being different from adjacent layers. The energy gap was somewhat reduced due to the 'tails' of the density of states in the compensated material. In this case, the active region played the role of a potential well, in which diffusion is partially restricted by a barrier produced by doping. Semiconductor heterobarriers serve as a tool for the confinement of carriers and photons in a specified active volume. It was shown in paper [51] devoted to the optimisation of the active-layer thickness in a heterolaser that, if the gain increases rapidly enough with the carrier concentration, it is appropriate to decrease the active-layer thickness (down to the then technologically accessible limit $\sim 20 - 50$ nm). This was the first recommendation to use ultrathin active layers, which was later realised in quantum well structures. The creation and study of lasers with ultrathin active layers was reported in paper [57]. The lasing threshold was significantly decreased in SCHs [58].

The volume rate of creation of excess carriers injected into a layer of thickness d is determined by the density J of

the injection current and is equal to $J/(ed)$, where e is the electron charge. For $d < L$, this rate can be assumed uniform over the depth, which results in the dependence of the threshold current density on the active-region thickness. By using a linear approximation for the recombination of carriers, we consider, for example, how the p–P-heterobarrier enhances the efficiency of using injected carriers. If the barrier is high enough in order to prevent the diffusion of electrons into the P-region, then the electron distribution will take the form $N_e(x) = N_{e0}\cosh[(d-x)/L]/\sinh(d/L)$. Here, we neglected the surface recombination at the p–P interface, assuming that the interface contains no defects. In this case, the average concentration in the active layer increases compared to that for free diffusion by a factor of $\gamma = 1/[1-\exp(-d/L)]$, which amounts to ~ 10 for $d/L = 0.1$ and ~ 100 for $d/L = 0.01$. Such an advantage is achieved already in a single heterostructure [51], where an optical mode is weakly confined within the active volume because of the dielectric asymmetry of the structure. This advantage was obtained in full measure in DHs and SCHs.

Because the penetration depth of the wave functions of carriers to barriers increases with decreasing the quantum-well width, the volume (3D) concentration of carriers in an ultrathin active layer looses its exact meaning when the volume localisation of carriers becomes greater than the nominal thickness d of the low-energy-gap active layer. The two-dimensional concentration N_{2D} has an exact physical meaning. The localisation region of carriers is determined in fact by the profiles of the probability density of the corresponding wave functions, which depend not only on the thickness but also on the principal quantum number, the effective mass, and the height of barriers. Nevertheless, the 3D concentration is very often used in calculations of quantum wells (to simplify comparison with a 3D case). For example, the effective 3D concentration is often used in calculations of the material gain g of a medium. This concentration is related to the 2D concentration by the expression $N_{3D} = N_{2D}/d$. To calculate the mode gain, it is necessary to determine the optical confinement factor Γ also related to the thickness d rather than to the size of the localisation region of carriers. In this case, $g_{mod} = g\Gamma$. This formally incorrect calculation gives sometimes a reasonable result, because, if carriers are localised within a layer of thickness $d^* > d$, then their concentration should be corrected by decreasing it proportionally to the ratio d/d^*, while the value of Γ should be corrected by increasing it by a factor of d^*/d. If, however, the material gain increases linearly with the carrier concentration, the product remains constant. This is true as long as the intensity of the electromagnetic field can be considered invariable within the active layer (which is the case for typical quantum wells) or within a packet of quantum wells in multilayer quantum well structures. This trick can be obviously used only for estimates but not in accurate calculations.

There are also crystallographic and technological restrictions on the minimum thickness of a quantum well. The thickness of a crystallographic monolayer in the (001) GaAs structure is 0.28 nm, and a deep localisation of carriers in such a well is no longer possible. The jumps in the thickness caused by the fabrication technology can be of the order of a monolayer thickness. The average thickness of the well typically greatly exceeds the monolayer thickness.

Quantum-size effects. Quantum-size effects in the context of this paper are the specific properties of the motion of carriers in extremely small volumes, which are comparable with (or less then) the wavelength of an electron or a hole. At the same time, these volumes should be large enough for the concepts of the band theory, such as the energy gap and the effective mass, to be applicable.

The layer of a low-energy-gap semiconductor located between higher-energy-gap semiconductors represents a potential well for carriers at least of the same sign. If the so-called heterojunction of the first type is formed between the semiconductors, the potential wells are formed for carriers of both signs (unlike heterojunctions of the second type, where the carriers are separated to different sides of the heterojunction). Upon localisation of the carriers, discrete allowed energy levels appear in the quantum well, and the lower (ground) state is characterised by the kinetic localisation energy (or simply localisation energy), which separates the corresponding ground level from the bottom of the potential well. In addition, the selection rules for radiative transitions in quantum wells also change, so that certain polarisations of radiation can be dominant and the divergence of radiation also can change somewhat.

Therefore, the energy of transition between the ground states in a quantum well proves to be greater than the energy of the interband transition in the same material. This gives an additional possibility to vary the wavelength of laser emission by varying the size of the quantum well, because the localisation energy in a square potential well with infinite barriers is $E_0 = \pi^2\hbar^2/(md^2)$, where m is the effective mass of a carrier. This expression gives good approximation for sufficiently deep potential wells. The correction for a finite depth of the well becomes important for levels located near the barrier edge.

The minimal thickness d_{min} of the well, at which the localisation of carriers is no longer provided, can be estimated from the inequality $E_0 \geqslant \Delta E$, where ΔE is the depth of the well. The estimate of d_{min} in GaAs and related materials gives $4-5$ nm, and in GaN about 2 nm. In thinner wells, the lower level is ejected from the well to a continuum. Strictly speaking, a bound state always exists in a quantum well; however, of practical importance are only the states that are sufficiently deep rather than the states that are easily thermally ionised.

Discretisation of the spectrum results in the change in the energy distribution of the density of states. The possibility to control the density of states provides a resource for further improvement of laser parameters. The matter is that, obviously, to obtain lasing, it is quite sufficient to produce inversion for working levels, i.e., for those levels in the bands that provide in fact the threshold amplification and the required rate of stimulated transitions upon pumping above the threshold. In semiconductors, it is also necessary to fill some levels in the bands, which are not directly involved in lasing. A usual (non-stimulated) recombination of these levels enters the expression for threshold losses. These levels are located either below or above the working levels. The lower levels should be filled because they themselves do not provide a sufficient gain, and a more powerful pumping is required to increase the gain. In a bulk semiconductor, the density of states increases approximately as the square root of the kinetic energy, so that there always exist 'non-working' levels in it that are located to the red

from the laser line. In a quantum well, the density of states increases abruptly, and if it is sufficient for obtaining the required gain, there is no in fact 'non-working' levels.

As for the levels that are located above the working levels, their population is determined by the temperature broadening of the quasi-equilibrium occupation function. The number of carriers at these levels corresponds to the integral of the product of the density of states by the occupation function for the specified energy interval. The occupation function is determined by the position of the Fermi quasi-level and temperature. The density of states of quantum wires and dots decreases with the energy exceeding the quantum level, so that the appropriate optimisation of the energy spectrum allows one to decrease in principle the contribution from non-working states lying above the working level. If a higher (next) quantum level is located far (much more than kT) from the ground level, then the tail of the occupation function broadens with increasing temperature to the region of low or (in the ideal case) zero density of states. This means that the temperature dependence of the gain and the lasing threshold can be in principle substantially reduced in such laser media.

The use of quantum effects in nanostructures for reducing the lasing threshold in semiconductor lasers mainly consists in the optimisation of the profile of the density of states. Sometimes, this is called 'the band engineering'. Note that this field was evolved simultaneously with the development of technology of strained heterostructures. The effect of the profile of the density of states on the threshold current and its temperature dependence was considered as early as 1960s. The advantage of reduced-dimension structures was analysed in papers [59, 60]. In fact, the temperature dependence of the gain weakens in the situation, which can be called a strong degeneracy. The criterion of a strong degeneracy in a bulk semiconductor is described by the inequality $F - E_c \gg kT$, where F is the Fermi quasi-level for electrons (the expression for holes is similar). In [61], a generalised criterion for a strong degeneracy was obtained for different (smooth) profiles of the density of states $\rho(E)$ in the vicinity of the Fermi level:

$$\frac{\mathrm{d}\ln\rho}{\mathrm{d}E} \ll \frac{1}{kT}. \qquad (1)$$

Expression (1) was used in paper [60] to analyse the threshold current in quantum well structures. It was shown that this condition is quite easily fulfilled in reduced-dimension nanostructures, for example, the density of states lying above the ground state in a quantum well is constant at all within a certain energy interval (between the ground and the first excited states). This means that the left-hand side of inequality (1) vanishes [inequality (1) is all the more fulfilled if its left side is negative]. The contribution to the temperature dependence is determined, however, by the presence of the part of the spectrum of the density of states where inequality (1) is not satisfied.

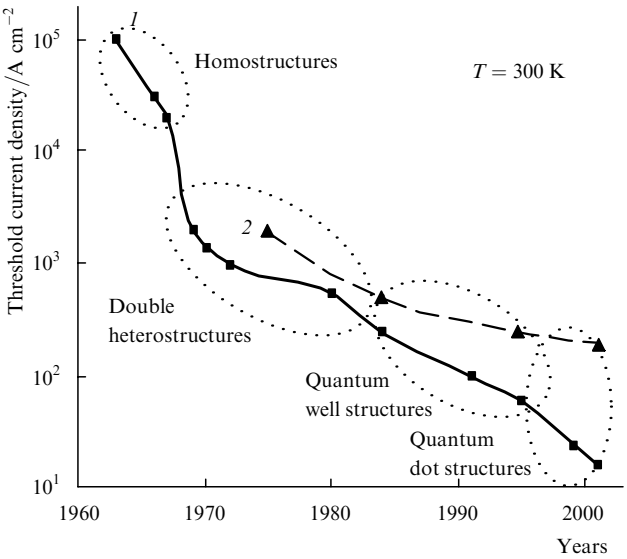

Figure 1. Evolution of the threshold current density at room temperature in injection lasers of different generations: (*1*) GaAs-based structures; (*2*) InP-based structures.

8. Evolution of the threshold current density and the threshold pump power density

Usually, a change in the threshold current or threshold current density is considered (Fig. 1). The threshold pump power density (per unit of an active volume) is also worth noting because this quantity characterises most adequately an excited state of the medium. Some estimates concerning the evolution of the threshold parameters of lasers based on the GaAs technology are presented in Table 1. It will be unexpected for many that, despite a drastic reduction of the threshold current density, the power density per unit

Table 1. Comparison of the threshold current density and the threshold pump power density in semiconductor lasers of different types (f is the filling factor equal to the ratio of the volume of quantum dots to the quantum-well volume).

Laser type	Active region thickness d/nm	Threshold current density J_{th}/A cm^{-2}	Voltage across the active region U/V	Pump power density p/W cm^{-3}
Epitaxial homolasers	>2000	20000	1. 5	$< 1.8 \times 10^8$
SHS	1500	10000	1.5	0.8×10^8
DH	100	1000	1.5	1.5×10^8
SCH QW	10	100	1.5	1.5×10^8
Quantum dot heterolasers ($f = 0.05$)	$10f$	10	~ 1.0	$(1/f) \times 10^7$ $\sim 2 \times 10^8$

Note: the active material for lasers of the first four types is GaAs and for the laser of the fifth type – InAs quantum dots in GaAs or InGaAs matrices; $d > 2000$ nm, as estimated from the diffusion length of electrons in GaAs.

volume remains almost invariable. This means that this progress was mainly achieved due to a decrease in the active-material volume per unit area of the p – n junction, whereas quantum effects themselves are of minor importance.

9. Point-centre semiconductor lasers

The development of the technology of reduced-dimension structures resulted in the creation of the quantum dot and quantum wire semiconductor lasers. Such lasers can be considered as intermediate devices between doped dielectric lasers and semiconductor lasers. They combine a number of positive properties inherent in lasers of both these types.

Quantum dots have an almost discrete energy spectrum. The narrower and more isolated their spectral lines, the weaker their temperature sensitivity, from which other semiconductor lasers are suffered. Indeed, when the spectrum is discrete, the emission band is not broadened with increasing temperature, as is the case of semiconductors, resulting in a stable gain. In addition, theoretically, the radiative lifetime of the excited zero-dimensional state is independent of temperature, whereas in a bulk semiconductor this lifetime noticeable increases with temperature. This leads usually to the temperature quenching of radiative recombination. The temperature stability of quantum dot lasers can be improved in principle to achieve that typical for ruby or neodymium lasers.

On the other hand, quantum dot lasers are pumped by low-voltage currents, which is typical for semiconductor injection lasers. In addition, quantum dot lasers are quite compact, economical and durable. Finally, quantum dots are very interesting objects of semiconductor physics.

Lasers on impurity centres in semiconductors also should be included to the family of dot centre semiconductor lasers. Shallow impurity levels in GaAs (especially in heavily doped materials) are involved in lasing. However, at present such lasers have no practical importance because one can manage quite well with undoped semiconductors.

Deep impurities. Deep impurities in semiconductors have not found applications so far, however, some recent progress can be observed. Interest in these studies is stimulated by the necessity of creation of silicon-based radiation sources because the nondirect-gap energy level diagram of a silicon matrix does not affect in principle strongly localised impurity centres. For this reason, lasing can be obtained in impurities in silicon, whereas attempts to obtain lasing at interband transitions have not met with success. Rare-earth impurities are also being actively studied in GaN, GaAs, and InP. All these materials exhibit injection luminescence observed upon radiative transitions in rare-earth ions. It seems that the inverse population can be readily produced in such centres because the excited-state lifetime of rare-earth impurity ions in semiconductors is ~ 1 ms. For the impurity concentration of 5×10^{18} cm^{-3} and a layer thickness of 1 μm, a pump density of ~ 0.08 A cm^{-2} is sufficient for populating the upper working state.

If such lasers were created, they would have a very low threshold. However, lasing is hindered by a very low effective gain cross section ($10^{-18} - 10^{-21}$ cm^2), which is typical for impurities. Because of such a low gain, even complete inversion cannot provide the amplification that would be sufficient for lasing. For example, if the cross section is 10^{-19} cm^2 and the concentration of inverted centres is 0.5×10^{18} cm^{-3}, then the maximum optical gain is 0.5 cm^{-1}, which is too low for semiconductors because the background (nonresonance) absorption by free carriers and defects is usually higher than this value. It is pertinent to make a comparison with an erbium-doped fibre amplifier, which is widely used in long-range communications and provides a gain of 20 – 30 dB for the amplifier length of 1 m and above. It is known that the background absorption in optical fibres at a wavelength of 1.54 μm where the amplifier operates is negligibly small, less than 1 dB km^{-1}. A gain of 0.5 cm^{-1} is sufficient for obtaining at a length of 1 m the amplification (unsaturated) above 200 dB! However, such a gain is insufficient for semiconductors, because the typical cavity length of commercial semiconductor lasers is too small, being of about 0.5 mm.

Nevertheless, the observations of some features of stimulated emission in semiconductors doped with erbium, although not lasing, were recently reported in several papers [62 – 65]. The first problem to be solved is to obtain the highest possible concentration of erbium, whose solubility in single-crystal semiconductors is low ($\sim 10^{18}$ cm^{-3}). According to [62], silicon nanocrystals can be doped with erbium up to concentrations $\sim 10^{20}$ cm^{-3}, while amorphous silicon can be doped with erbium up to 2.5×10^{20} cm^{-3} [63]. Note that we have to deal with optically active impurities, whereas in the case of heavily doped materials, some impurities (for example, precipitated or in clusters) become optically inactive.

The solubility of erbium in single crystals is much lower, however, due to the optimisation of simultaneous doping of GaAs with erbium and oxygen, the concentration of erbium can achieve $\sim 8 \times 10^{18}$ cm^{-3} [64]. At low temperatures, the GaAs : Er,O/InGaP heterostructures exhibited the properties of stimulated emission in a narrow 1538-nm line [64]. The excitation mechanism involved the trapping of excess carriers by local Er-2O centres followed by the energy transfer to the inner f shell of the Er ion. Because the excited-state lifetime of erbium is ~ 1 ms, the population inversion at the $^4I_{13/2} \rightarrow {}^4I_{15/2}$ transition can be obtained at a comparatively low pump rate. At room temperature, the conditions for stimulated emission worsen because nonradiative losses increase and the luminescence lines of Er ions broaden.

Quantum dot and quantum dash lasers. The theoretical analysis of a semiconductor quantum size object (a sphere of a small radius) was initiated in papers [66 – 68]. The reduced-dimension objects, such as quantum dots and wires, can be treated as molecule-like objects because their energy spectrum should be calculated quantum-mechanically taking into account the properties of solids. The approach, known as the effective mass method, often proves to be adequate. In this case, the Schrödinger equation is in fact used twice: first the crystal field of homogeneous materials is considered, which allows us to determine the energy bands of a semiconductor and the effective masses of carriers. Then, assuming that the band edges correspond to the potential energy of carriers, we again solve the Schrödinger equation for carriers in 'quantum wells' taking into account a new (smoothed) profile of the potential energy in order to find a new position of energy levels or mini-bands, as well as other parameters. Because the quantum size restriction leads to a

substantial shift of the energy levels, the formation of such structures results in the appearance of new spectral ranges where the laser emission can be tuned.

A solid atom-like object features the following properties. First, the polarisation of a solid substantially reduces Coulomb forces, thereby lowering the ionisation energy of a hydrogen-like centre by a factor of ε^2, where ε is the relative permittivity of the medium (because $\varepsilon \simeq 13.3$ in GaAs, the ionisation energy decreases by a factor of 177). Second, the motion of carriers depends on the effective mass. A simultaneous consideration of polarisation and the effective mass in GaAs results in the increase in the Bohr radius from 0.0529 nm in a hydrogen atom to ~ 10 nm in hydrogen-like dot centre in GaAs. Because a sphere of such a radius contains about 2×10^5 atoms, the effective mass approximation is valid. Nevertheless, elements of size ~ 10 nm prove to be 'atom-like' in this solid matrix. If we take for comparison the material parameters such as the de Broglie wavelength and the mean free path of carriers, the former for a thermal electron in GaAs is 24 nm at room temperature, while the latter can be $50 - 150$ nm (being strongly dependent on the material quality). Therefore, the elements of size of the order of 10 nm and smaller represent quantum size objects in GaAs.

It seems that, along with objects having a strictly definite dimension, the elements with an intermediate dimension can also exist, such as wires covering a plane, dots forming lines, and 'dashes' having a dimension that is intermediate between the one- and zero-dimensional elements.

Note that the geometry of reduced-dimension structures deviates from perfect. We pointed out in paper [69] that the side profiling in real semiconductors is not necessarily complete, i.e., with a complete separation of individual elements. It is known now that quantum dots represent in fact thickenings located on the so-called wet layer, which consists of the same material as quantum dots, but covers continuously a substrate. The solution of the Schrödinger equation for such structures showed that the deepest states reproduce the properties of reduced-dimension elements without the necessity of a complete separation of these elements. Moreover, the corresponding energy levels of the states created by the wet layer are located high enough above the ground states of quantum dots not to affect the properties of the device.

Modern technological methods provide rather high spatial resolution in the manufacturing of semiconductor structures. As is known, first (approximately beginning from 1970) attempts in this direction were concentrated on the improvement of control of the growth process in order to achieve the quantum-size limit at least in one (vertical) dimension. The precision technologies of epitaxial growth such as molecular-beam and metalorganic vapour phase epitaxy, which allow one to control the growth of atomic monolayers, have played a key role in these studies. These technologies are now used for commercial production of quantum well structures.

To reduce the dimension of quantum well structures further, it was necessary to develop the technology of side restriction with an ultrahigh spatial resolution. The problem to be solved was to profile the potential energy of carriers in side directions with typical dimensions less than 100 nm. A direct and quite costly method is precision photo- and cathodolithography. In this case, first a semifinished structure with ultrathin layers is grown. Then, the side-restricted lithographic formation of the structure is performed to produce the elements of quantum wires (one-dimensional elements) or quantum dots (zero-dimensional elements). Then, the profiled structure is overgrown with higher-energy-gap materials, completing the two- or three-dimensional confinement. For example, laser structures with overgrown InGaAs stripes of width 30 nm and period 70 nm were fabricated by etching and epitaxial closure [70].

Quantum wires are also fabricated by growing multilayer quantum size structures on a nonplanar substrate with preliminary precisely etched grooves [71, 72]. Sometimes the side profiling is achieved in structures with 'stressors' – quantum size stressed elements, which are located outside the initial quantum well but close enough to it in order to modulate the position of band edges due to elastic deformation. Another method for manufacturing periodic lateral confined quantum size structures is the growing of ultrathin layers on the vicinal plane of a substrate, i.e., on the plane containing crystallographic (almost periodical) steps due to a small deviation from orientation with respect to the low-index plane [73]. The review of studies on quantum wire lasers is presented in [74].

Precision lithography was used for the fabrication of periodic quantum size all-round confined structures (regular quantum dot networks) [75, 76]. In [76], quantum dots in the form of InGaAs quantum well islands of diameter ~ 30 nm and step 70 nm were produced using cathode-ray lithography and liquid-phase etching. Lasing was obtained at a wavelength of 1.26 μm at 77 K (the threshold current density was ~ 1 kA cm $^{-2}$.

A greatest progress in the manufacturing of quantum dot structures was achieved by using the self-formation of extremely small elements. When an epilayer and a substrate are substantially mismatched, crystallisation proceeds via the so-called Krastanov–Stransky mechanism, resulting in the formation of two-dimensional islands at the initial stage instead of homogeneous layers. If the rate of deposition and thickness of the epilayer are accurately controlled, these islands form a comparatively homogeneous ensemble of nanometre elements. This occurs due to the minimisation of the total energy of nucleation centres, which includes the elastic energy of the mismatch of the lattices. The formation of nanoislands proves to be energetically profitable when the amount of the deposited material is small. This amount usually corresponds to several (for example, two) monolayers of the deposited material (which is determined by averaging over the entire area). Atomic-force microscope photographs show that the nanoislands have the shape of pyramids and cones. The dot density is usually varied from 3×10^{10} to 10^{11} cm^{-2}, while the average diameter of cones is $10 - 20$ nm and their height is $5 - 10$ nm. The mutual arrangement of self-formed quantum dots is not periodic and irregular, and is determined only by a correlation appearing due to a competition for a material. The size of individual elements noticeably fluctuates about their mean values, resulting in the inhomogeneous broadening of the corresponding energy spectra. Nevertheless, the self-formation of quantum dots eliminates the necessity of 'drawing' each dot lithographically, thereby substantially simplifying and lowering the cost of their fabrication. A detailed review of studies of quantum dot structures is presented in [77].

The self-formation of InAs or InGaAs islands upon crystallisation on a GaAs substrate was observed in papers

[78 – 80]. Then, many studied were performed in which the threshold current density was further decreased. Lasers with an extremely low threshold current density (~ 20 A cm^{-2}) at room temperature [81] were manufactured by optimising a quantum size SCH and a system of quantum dots itself. The quantum dots were placed into a quantum well. For example in [81], InAs quantum dots were located in an InGaAs quantum well, which in turn was located inside a GaAs waveguide with AlGaAs emitter layers used as plates. The lasing threshold was observed in quantum dot lasers at current densities 90 [82], 85 [83], 26 [81], and 16 A cm^{-2} [84]. The minimum threshold current in VCSELs was 286 μA [85] for the active region volume estimated as 4×10^{-14} cm^3.

In quantum dot lasers, a physical limit of the minimum volume of an active medium is achieved. The maximum optical gain decreases with decreasing the number of particles in the cavity. For this reason, long cavities ($1 - 2$ cm) or cavities with the high reflectivity should be used in the lowest-threshold quantum dot lasers. Otherwise, lasing was developed at higher levels, where the threshold current density was substantially higher. This does not mean that all the possibilities for reducing the threshold current density are exhausted. If all the types of losses of electron energy are eliminated, the limiting threshold current density should be as low as ~ 1 A cm^{-2}.

The geometry of nanoislands formed during the growth of quantum size structures is somewhat subjected to the influence of the anisotropy of the two-dimensional diffusion of atoms adsorbed on the crystallisation-front surface. In some systems, for example, when InAs is grown on InP, this anisotropy is so substantial that the islands have the shape of dashes rather than dots [85, 86]. Therefore, the spectrum of such elements has a high-energy tail of states, which is typical for quantum wires. The anisotropy of the gain and of other optical characteristics in quantum dash lasers was studied in paper [86].

Note that a laser usually operates at one or several modes. Therefore, emission at non-lasing modes is lost. For this reason, the anisotropic emission of active particles, which should be properly oriented for emitting at the required mode. Quantum wires and dashes undoubtedly offer such a possibility: because emitting dipoles in them are predominantly oriented along the longitudinal axis of an object, they mainly emit at the mode for which a laser beam is directed perpendicular to wires or dashes.

10. Spectral threshold characteristic

There exists a natural relation between the threshold current density and the photon energy at the lasing threshold in semiconductor lasers, which is called the spectral threshold characteristic. This characteristic shows that the lasing frequency is not constant even for laser diodes of the same type and depends on the threshold current density (for example, because of the difference in cavity lengths or reflectivity of mirrors). Fig. 2 shows such characteristics for lasers of several generations [61, p.251]. The characteristics of the last generation of lasers, quantum dot lasers, are presented in Fig. 3. Their specific feature is a discontinuity, which is caused by the quasi-discrete energy spectrum of the active medium. One can also see that within the band of transition of the same type, the curves exhibit a slope, which is determined by the density of states occupied to obtain the gain at the laser frequency.

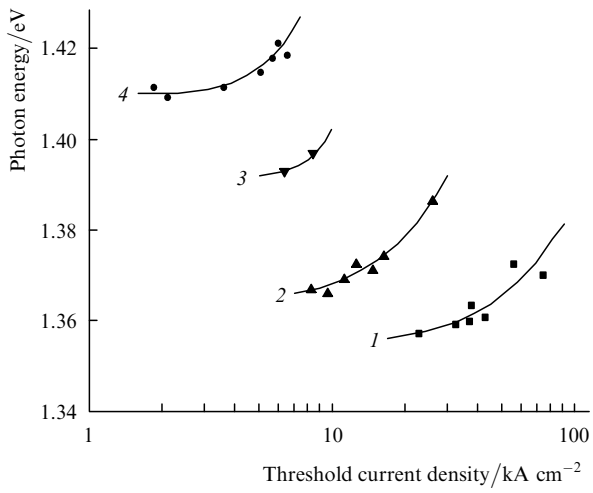

Figure 2. Spectral threshold characteristics of GaAs lasers: (*1*) heavily doped GaAs homolasers; (*2*) single AlGaAs/GaAs heterostructures (the active region is a compensated p-GaAs of thickness 2 μm); (*3*) double AlGaAs/GaAs heterostructures (the active p-GaAs region of thickness 0.8 mm); (*4*) double AlGaAs/GaAs heterostructure (the active n-GaAs region of thickness 0.8 μm) [61].

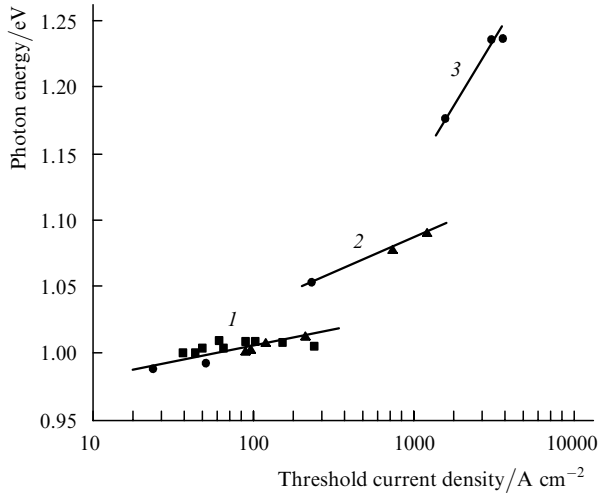

Figure 3. Spectral threshold characteristics of lasers on InAs quantum dots in an InGaAs quantum well on a GaAs substrate [84]: (*1*) ground-state band (transitions between the ground states of electrons and holes in a quantum dot); (*2*) first 'excited' band; (*3*) second 'excited' band.

11. Lasing efficiency

Initially, it was expected that semiconductor lasers would have a high efficiency because there were no principal reasons preventing the efficiency of about 100 %. However, a high lasing efficiency could not be obtained experimentally because of the high threshold current at room temperature. Nevertheless, the efficiency of GaAs homolasers at liquid nitrogen temperature was ~ 25 % [87]. In one of the earlier papers on the optimisation of the cavity of laser diode for obtaining the maximum optical cw power at room temperature [88], all the internal parameters of lasers available at that time (1970) were taken into account, as well as the possibility of heat removal, because the overheating of the active region during cw lasing restricts

the output power. The maximum output power above 1 W was obtained, in good agreement with that predicted in modern lasers (5 – 10 W for a diode). On the other hand, the efficiency calculated for the maximum-power regime did not exceed 6.5 %, which was explained by low values of the internal parameters used in the calculation. For example, since then the threshold current density was reduced by 50 – 60 times, and the coefficient of internal losses was reduced at least by a factor of ten.

Modern laboratory semiconductor lasers have the conversion efficiency 60 %–70 % at room temperature. Commercial lasers used for pumping solid-state lasers have the efficiency of 45 %. Consider now physical restrictions imposed on the efficiency of a laser diode.

Energy yield. One of the principal restrictions is the energy yield η_E, which represents the averaged ratio of the photon energy to the energy spent for producing one electron-hole pair (a pair of carriers in the active medium is meant; the leakage of the pump current is neglected in the calculation). The laser photon energy $E = h\nu$ is defined very accurately. The energy spent to produce the electron-hole pair includes the average energy of the pair of carriers, which is determined by the difference ΔF of Fermi quasi-levels. During lasing, the condition $\Delta F > h\nu$ must be fulfilled, therefore, the value of $\eta_E = h\nu/\Delta F$ is always smaller than unity. After each event of stimulated emission at the laser frequency, a pair with the energy lower than the average energy is excluded from an ensemble of pairs with different energies. Formally, this means that the electron-hole gas is heated and then passes to the initial equilibrium state, by transferring heat to a crystal lattice. Unlike the lasing regime, thermodynamics in the LED regime does not forbid the opposite situation, when $h\nu > \Delta F$, so that a lattice is cooled upon emission, and the emission efficiency can in principle exceed 100 %.

The difference between ΔF and $h\nu$ during lasing can be approximately equal to the thermal energy kT. Therefore, the upper limit of the energy yield is estimated as $1 - kT/h\nu$. For example, $\eta_E = 98.2\,\%$ for a GaAs laser emitting at 1.4 eV at room temperature. It is obvious that this restriction in long-wavelength lasers is stronger. Thus, the upper limit of η_E is $\sim 80\,\%$ for a laser emitting at 10 μm. This means that the laser temperature should be decreased for obtaining the highest efficiency.

Along with ΔF, the terms caused by thermalisation of carriers can contribute to the energy spent for producing one electron-hole pair. In the case of one-photon optical pumping, the energy yield is determined by the relation $h\nu/h\nu_{\rm p}$, where $h\nu_{\rm p}$ is the pump photon energy, i.e., the energy yield contains all the losses related to the photon defect energy, including thermalisation of carriers. Upon pumping by an electron beam, the maximum energy yield $\sim 30\,\%$ is restricted by thermalisation losses. Upon injection to the p – n junction, the heating and subsequent thermalisation of carriers can be avoided because the injection is reduced to the diffusion of carriers, which does not assume the deviation from the condition of their quasi-equilibrium. This means that in p – n junctions the most economical pumping methods is used among those existing in quantum-electronic devices.

The energy of injected carriers in the active region of heterostructures can exceed ΔF because the carriers transfer to its working states by trapping from higher states. The energy released upon trapping is spent finally to heat the lattice. This energy corresponds approximately to the total height ΔE of barriers lmiting the active region. To perform the electron confinement, the height of barriers should be equal at least $4kT$. It seems that the reasonable value of the total height ΔE for carriers of both signs is $\sim 8kT$. Therefore, the real value of the energy yield is $\eta_{E_{\max}} = 1 - (\Delta E + kT)/h\nu \approx 1 - 9\,kT/h\nu$, which gives the efficiency $\sim 84\,\%$ equal to that for a GaAs laser.

We can introduce the generalised energy yield as the ratio $h\nu/eV$, where V is the voltage applied to a diode from the mains. In this case, the losses include the energy spent for the drift of carriers in wires, contacts, and passive regions of the diode. To measure the lasing efficiency, we should calculate an overall quantum efficiency of the laser, i.e., the ratio of the number of laser photons to the number of carriers passing through the diode cross section upon pumping. The quantum efficiency takes into account quantum losses related to the carrier leakage and the intracavity reabsorption of photons. The product of the energy yield by the total quantum efficiency is the lasing efficiency. Electric losses are often calculated separately, by separating the efficiency of the p – n junction and the total efficiency of the device.

Electric (Joule) losses are also inevitable if external materials are not superconductors. They can be minimised by using low-resistance contacts and passive regions; however, they increase with increasing current I as $I^2 R_{\rm s}$, where $R_{\rm s}$ is a series resistance of the diode (after exclusion of the nonlinear resistance of the p – n junction). During lasing high above the threshold, $R_{\rm s}$ corresponds approximately to the differential resistance of the diode. It is Joule losses that impose the principal restriction on the lasing efficiency in the high-current limit (which is sometimes cannot be achieved in experiments for different reasons).

The electronic quantum efficiency is restricted by the following reasons.

(1) When the lasing threshold is achieved, only a part of excess carriers are involved in stimulated recombination, whereas the remaining part recombines spontaneously and nonradiatively. Because above the lasing threshold the concentration of excess carriers almost does not change, the threshold losses related to spontaneous emission and nonradiative recombination (if any) prove to be inevitable. The higher the threshold current density, the higher these threshold losses. The lasing efficiency at the threshold is zero, and to obtain the high efficiency, the pump power should greatly exceed the lasing threshold. The differential quantum efficiency is introduced to describe lasing and it corresponds to an increase in the number of photons with respect to the number of carriers injected to the active region for the same time.

(2) The gain saturation (the condition of a steady-state lasing) results in the saturation of the concentration N of excess carriers, if, as usual, the gain and N are unambiguously related with each other. However, this unambiguity is violated during lasing, and the gain changes somewhat depending on the photon density (nonlinear gain occurs). A decrease in the gain (for N specified) is automatically compensated by an increase in N. Therefore, the threshold level of recombination losses and, in particular, the intensity of spontaneous emission increase simultaneously. A small relative addition to the recombination rate in the linearised form is $\varepsilon_{\rm nl} N_{\rm ph}$, where $\varepsilon_{\rm nl}$ is the nonlinear gain and $N_{\rm ph}$ is the photon density. The empirical value of $\varepsilon_{\rm nl}$ is approximately

10^{-21} cm^3 and the photon density achieves $\sim 10^{16}$ cm^{-3}. Therefore, the relative increase in threshold losses is $\sim 10^{-5}$, i.e., it is rather small.

(3) An incomplete overlap of a region being pumped with the mode volume can be caused by the material inhomogeneity (typical for laser diodes of the first generation) and by an insufficient side confinement (current leakage and diffusion of carriers into passive regions). In addition, the overlap can change with increasing pump power because of a change in the mode volume: the deformation and switching of dominant modes and filamentation caused by optical nonlinearity (self-focusing). To put it very simple, if the pump current flows in regions where the laser field is weak or absent, the pumping efficiency will be lower than 100 %. Effects caused by the uniform consumption of the energy of excess carriers over the active region length (spatial hole burning) can be weakened to a some extent by using a medium with a low optical nonlinearity (the low amplitude-phase coupling) and reducing the electric resistance of passive regions adjacent to the active region [89, 90].

(4) Because excess carriers can be ejected from working states to barrier layers due to thermal ionisation and a finite residence time of carriers in barrier layers before there are trapped in the working states, a 'parasitic' recombination takes place (which does not contribute to stimulated emission) outside the active region. If the recombination includes radiative recombination, the latter produces emission at frequencies lying, as a rule, far from the laser frequency. These losses are typical for structures with the step-by-step trapping of carriers to the working states. For example, excess carriers in quantum dot lasers are injected into the 'waveguide' layers of the heterostructure, then are trapped in a quantum well, and only thereafter they are trapped in the working states in quantum dots. In both intermediate states, the concentration of carriers is finite. In the general case, this concentration increases with the pump power (whereas the concentration of carriers in the working states increases slowly due to the gain saturation, as mentioned above). The rate of 'parasitic' recombination of excess carriers in the intermediate states increases with their concentration, resulting in the increase of losses, which restrict the output power and reduce the slope of the output characteristic. The pumping losses at the stage of trapping of carriers can be estimated from the ratio of the recombination rate to the trapping rate in a given intermediate state. If the concentration of carriers is N, then the recombination rate can be written in the form $R = AN + BN^2$, where A is the linear recombination coefficient and B is the quadratic (radiative) recombination coefficient. The trapping rate is $C = N/\tau_c$, where τ_c is the trapping time. In the case of trapping of carriers from a barrier layer by a quantum well, we can use the diffusion estimate of the trapping time: $\tau_c = d_b^2/D$, where d_b is the barrier-layer thickness and D is the diffusion coefficient of carriers. Then, the pumping efficiency is

$$\frac{C}{C+R} = \frac{1}{1+\tau_c(A+BN)}.$$

One can see that the pumping efficiency decreases with increasing N, which can be manifested in a sublinear behaviour of the light-current characteristic of a laser. To make a numerical estimate, we will use parameters close to those for GaAs ($d_b = 100$ nm): $A = 10^9$ s^{-1}, $B = 2\times 10^{-10}$ cm^3 s^{-1}, $D = 10$ cm^2 s^{-1}. As a result, we obtain, for the useful current of density 10 kA cm^{-2}, $\tau_c = 10$ ps and the trapping efficiency ~ 99 %. Although these restrictions seem unimportant, however, the corresponding losses increase with increasing pump power and temperature (due to thermal emission of trapped carriers).

The optical quantum efficiency is the ratio of the integrated output photon flux in a laser beam to the number of photons generated in the cavity per unit time. Photon losses can be caused by the nonresonance reabsorption of photons and by the escape of photons from the cavity due to scattering. The decay of laser radiation in the cavity is described by the internal loss factor α. The near-threshold efficiency of radiation outcoupling is described by the expression $f_{out} = \ln(1/R)/[\alpha L + \ln(1/R)]$, where L is the cavity length; $R = (R_1R_2)^{1/2}$; R_1, and R_2 are the reflection coefficients of the mirrors of a Fabry–Perot resonator. The parameters of the resonator should be optimised. Thus, to obtain a sufficiently low lasing threshold, the values of L, R_1, and R_2 should be increased, while to obtain a high lasing efficiency, they should be decreased. One can see that, for the given value of α, an increase in the cavity length should not exceed $\sim 1/\alpha$ because otherwise the lasing efficiency is reduced. In modern lasers, $\alpha = 1 - 5$ cm^{-1}, which corresponds to the maximum cavity length $2 - 10$ mm. In practice, the values $L = 0.5 - 1$ mm are used. For typical values $L = 0.5$ mm, $R_1 = 0.1$ (frontal facet) and $R_2 \approx 1$ (rear facet), we obtain $f_{out} = 0.92$ for $\alpha = 2$ cm^{-1} and $f_{out} = 0.96$ for $\alpha = 1$ cm^{-1}.

Let us calculate the radiation power P for a laser with the above parameters: $P = (h\nu/e)\eta_{int}f_{out}(I - I_{th})$, where η_{int} is the internal quantum efficiency and I_{th} is the threshold current. The internal quantum efficiency is introduced as phenomenological coefficient, which takes into account the electronic pump losses considered in this section. In [61], this quantity is called the pumping efficiency because it represents the ratio of the energy of electron-hole pairs in the active region to the energy spent to produce them. The lasing efficiency is defined as the ratio of the laser output power to the total electric power consumed, i.e., the lasing efficiency is P/IV, where I is the pump current and V is the voltage applied across the diode.

In a diode with a cavity length of 0.5 mm and width of 0.1 mm, the threshold current is approximately 0.1 A in a separate-confinement quantum well structure. For $f_{out} = 0.92$, $\eta_{int} = 1$, and $h\nu/e = 1.4$ V, a pump current of 760 mA is required to obtain an output power of 1 W. If a series resistance is 0.02 Ω and the voltage applied across the active region is 1.625 V, then the expected lasing efficiency is 70 %.

Table 2 presents some power characteristics for highly efficient laser diodes. One can see that the real lasing efficiency of laboratory lasers lies in the interval 25 %–66 %, i.e., it is close to the optimistic estimate made above, and achieves 45 % in commercial lasers. Note that this concerns multimode lasers. The efficiency of single-mode lasers can be somewhat lower, mainly because a single-mode lasing is usually achieved at a lower excess over the threshold. For example, the efficiency of a single-mode 200-mW SDL-5430 commercial laser tunable in the wavelength range from 810 to 852 nm is 30 %. If an optical scheme in which a laser diode is used has a restricting aperture, this can result in additional losses due to a strong

Table 2. Parameters of highly efficient laser diodes. The two last lines correspond to commercial lasers.

Laser type	T/K	λ/nm	α/cm^{-1}	P/W	Efficiency (%)	Year and reference
Diffusion p – n junction GaAs homolaser (pulsed regime)	77	850	10	30 – 50	25	1966 [88]
SHS GaAs/AlGaAs laser	300	900	–	1 – 5	40	1970 [91]
InGaAs quantum well heterolaser	300	1064	–	5.25	50 ($P = 1$ W) 30 ($P = 1$ W)	1991 [92]
InGaAs quantum well heterolaser	300	980	–	8.1	66 (maximum) 54 ($P = 3.7$ W) 43 ($P = 8.1$ W)	1996 [93]
Submonolayer quantum dot InAsGaAs heterolaser	300	937	3.2	6	58 – 59	2002 [94, 95]
SDL-6380-A InGaAs quantum well heterolaser	300	910 – 980	–	2 – 4	45	2002 [SDL web-site (USA)]
SDL-2470-A quantum well heterolaser	300	798 – 800 or 808 – 812	–	3	35	2002 [SDL web-site (USA)]

divergence of emission from laser diodes. For example, the efficiency of lasers coupled with optical fibres is 25 %.

Another important circumstance is the heating of the active region by the pump current. The estimates made above correspond to the 'isothermal' conditions under which the laser parameters were assumed constant and corresponding to the temperature of the active region. These parameters are substantially deteriorated at high temperatures. The development of various methods for efficient cooling is a separate problem. Note also that the role of heating becomes less important upon pumping by short pulses (of the order and shorter than the lifetime of carriers), however, spontaneous and nonradiative recombination occurring in periods between laser pulses will increase losses.

The use of highly efficient, high-power laser diodes is necessary and desirable for a variety of applications (for optical pumping of solid-state lasers, in industrial technologies, in surgery and ophthalmology) because their efficiency leads to a decrease in the dimensions and weight of power supplies, simplifies cooling systems, enhances the overall efficiency of devices, and reduced the energy consumption. In particular, the pumping of high-power industrial lasers by laser diodes drastically changes their design as the cost of diode laser arrays lowers: there is no need for clumsy high-voltage power supplies (typical for flashlamp pumping), water cooling becomes unnecessary, and problems related to thermal elastic distortions in solid active elements are simplified.

Semiconductor lasers are now widely used in a variety of modern devices and they live up to the hopes of their creators. A leading place among them belongs to Nikolai Gennadievich Basov, who laid the foundations of the physics of semiconductor lasers and made a great contribution to their development.

Acknowledgements. This work was partially supported by the 'Leading Scientific Schools' Program (Grant No. 00-15-96624).

References

1. Basov N.G., Vul B.M., Popov Yu.M. *Zh. Eksp. Teor. Fiz.,* **37**, 587 (1959).
2. Basov N.G., Krokhin O.N., Popov Yu.M. *Zh. Eksp. Teor. Fiz.,* **40**, 1879 (1961).
3. Hall R.N., Fenner G.E., Kingley J.D., Soltys T.J., Carlson R.O. *Phys. Rev. Lett.,* **9** (9), 366 (1963).
4. Nathan M.I., Dumke W.P., Burns G., Dill J.H. Jr., Lasher G.J. *Appl. Phys. Lett.,* **1** (3) 62 (1962).
5. Holonyak N. Jr., Bevaqua S.F. *Appl. Phys. Lett.,* **1** (4), 82 (1962).
6. Quist T.M., Rediker R.H., Keyes R.J., Krag W.E., Lax B., McWhorter A.L., Zeiger H.J. *Appl. Phys. Lett.,* **1** (4), 91 (1962).
7. Bagaev V.S., Basov N.G., Vul B.M., Kopylovskii B.D., Krokhin O.N., Popov Yu.M., Markin E.P., Khvoshchev A.N., Shotov A.P. *Dokl. Akad. Nauk SSSR,* **150**, 275 (1963).
8. Bolger B., Van de Does de Bije J.A.W., Kalter H., Vegter H.J. *Phys. Lett.,* **3**, 252 (1963).
9. Nasledov D.N., Rogachev A.A., Ryvkin S.M., Tsarenkov B.F. *Fiz. Tverd. Tela,* **4**, 1062 (1962).
10. Hall R.N. *IEEE J. Quantum Electron.*, **23** (6), 674 (1987).
11. Nathan M.I. *IEEE J. Quantum Electron.*, **23** (6), 679 (1987).
12. Holonyak N. Jr. *IEEE J. Quantum Electron.*, **23** (6), 684 (1987).
13. Rediker R.H., Melngailis I., Mooradian A. *IEEE J. Quantum Electron.*, **20** (6), 602 (1984).
14. Rediker R.H. *IEEE J. Quantum Electron.*, **23** (6), 692 (1987).
15. Alferov Zh.I., Kazarinov R.F. USSR Inventor's Certificate No. 181737 (1963).
16. Kroemer H. *Proc. IEEE*, **51** (12), 1782 (1963).
17. Alferov Zh.I., Andreev V.M., Korol'kov V.I., Portnoi E.L., Tret'yakov D.N. *Fiz. Tekh. Poluprovodn.,* **2**, 1545 (1968).
18. Basov N.G., Bogdankevich O.V., Devyatkov A.G. *Dokl. Akad. Nauk SSSR,* **155**, 78 (1964).
19. Basov N.G., Grasyuk A.Z., Katulin V.A. *Dokl. Akad. Nauk SSSR,* **161**, 1306 (1965).
20. Basov N.G., Molchanov A.G., Nasibov A.S., Obidin A.Z., Pechenov A.N., Popov Yu.M. *IEEE J. Quantum Electron.*, **13** (8), 699 (1977).
21. Basov N.G., Bogdankevich O.V., Grasyuk A.Z. *IEEE J. Quantum Electron.*, **2** (9), 594 (1966).
22. Andronov A.A. *Pis'ma Zh. Eksp. Teor. Fiz.,* **30**, 585 (1979); *Far-Infrared Semiconductor Lasers*. Ed. by E. Gornik, A.A. Andronov. *Spec. Issue of Opt. Quant. Electron.,* **23** (2) (1991).
23. Faist J., Capasso F., Sivco D.L., Sirtori C., Hutchinson A.L., Cho A.Y. *Science,* **264**, 553 (1994).
24. Capasso F., Gmachl C., Paiella R., Tredicucci A., Hutchinson A.L., Sivco D.L., Baillargeon J.N., Cho A.Y., Liu H.C. *IEEE J. Select. Topics Quantum Electron.,* **6** (6), 931 (2000).

25. Namjou K., Cai S., Whittaker E.A., Faist J., Gmachl C., Capasso F., Sivco D.L., Cho A.Y. *Opt. Lett.*, **32** (3), 219 (1998).
26. Akasaki I., Amano H., Sota S., Sakai H., Tanaka T., Koike M. *Jpn. J. Appl. Phys.*, **34**, L1517 (1995).
27. Nakamura S., Senoh M., Nagahama S., Iwasa N., Yamada T., Matsushita T., Kiyoku H., Sugimoto Y. *Jpn. J. Appl. Phys.*, **35** (1B), L74, (1996).
28. Nakamura S., Senoh M., Nagahama S., Iwasa N., Yamada T., Matsushita T., Kiyoku H., Sugimoto Y. *Appl. Phys. Lett.*, **70** (7), 868 (1997).
29. Nakamura S., Fasol G. *The Blue Laser Diode* (Berlin: Springer–Verlag, 1997).
30. Haase M.A., Qiu J., DePuydt J.M., Cheng H. *Appl. Phys. Lett.*, **59**, 1272 (1991).
31. Jeon H., Ding J., Patterson W., Nurmikko A.V., Xie W., Grillo D.C., Kobayashi M., Gunshor R.L. *Appl. Phys. Lett.*, **59**, 3619 (1991).
32. Nurmikko A.V., Gunshor R.L. *Physica B*, **185**, 16 (1993).
33. Shoen J.H., Kloc C., Batlogg B. *Science*, **288**, 2338 (2000).
34. Eliseev P.G. *Semiconductor Lasers II. Materials and Structures*. Ed. by E. Kapon (San Diego: Acad. Press, 1999) pp 71–155.
35. Eliseev P.G., Ismailov I., Man'ko M.A., Krasil'nikov A.I., Strakhov V.P. *Fiz. Tekh. Poluprovodn.*, **1**, 1315 (1967).
36. Basov N.G., Eliseev P.G., Ismailov I., Pinsker I.Z., Strakhov V.P. *Zh. Tekh. Fiz.*, **37**, 349 (1967).
37. Basov N.G., Eliseev P.G., Nikitin V.V., Lishina A.V., Maslov V.N., Nashel'skii A.Ya. *Fiz. Tverd. Tela*, **7**, 1902 (1965).
38. Butler J.F., Calawa A.R. *J. Electrochem. Soc.*, **112** (10), 1056 (1965).
39. Butler J.F., Calawa A.R., Harman T.C. *Appl. Phys. Lett.*, **9** (12), 427 (1966).
40. Panish M.B., Hayashi I., Sumski S. *IEEE J. Quantum Electron.*, **5** (4), 210 (1969).
41. Kressel H., Nelson H. *Appl. Phys. Lett.*, **15** (1), 7 (1969).
42. Dolginov L.M., Eliseev P.G., Libov L.D., Pinsker I.Z., Shevchenko E.G. *Kratk. Soobshch. Fiz. FIAN*, (9), 9 (1970).
43. Alferov Zh.I., Andreev V.M., Portnoi E.L., Trukan M.K. *Fiz. Tekh. Poluprovodn.*, **3**, 1328 (1969).
44. Alferov Zh.I., Andreev V.M., Garbuzov D.Z., Zhilyaev Yu.V., Morozov E.P., Portnoi E.L., Trofim V.G. *Fiz. Tekh. Poluprovodn.*, **4**, 1826 (1970).
45. Hayashi I., Panish M.B., Foy P.W., Sumski S. *Appl. Phys. Lett.*, **17** (3), 109 (1970).
46. Bronshtein I.K., Dolginov L.M., Druzhinina L.V., Eliseev P.G., Krasavin I.V., Libov L.D. *Kratk. Soobshch. GIREDMET, Ser. V*, (21) (1970).
47. Dolginov L.M., Druzhinina L.V., Eliseev P.G., Krasavin I.V., Libov L.D. *Kratk. Soobshch. Fiz. FIAN*, (2), 57 (1971).
48. Bogatov A.P., Dolginov L.M., Druzhinina L.V., Eliseev P.G., Sverdlov B.N., Shevchenko E.G. *Kvantovaya Elektron.*, **1**, 2294 (1974) [*Sov. J. Quantum Electron.*, **4**, 1281 (1974)].
49. Eliseev P.G. Preprint FIAN, (33) (Moscow: 1970).
50. Dolginov L.M., Eliseev P.G., Libov L.D., Pinsker I.Z., Portnoi E.L., Kharisov G.G., Shevchenko E.G. *Kratk. Soobshch. Fiz. FIAN*, (12), 63 (1970).
51. Eliseev P.G. *Kratk. Soobshch. Fiz. FIAN*, (4), 3 (1970).
52. Kirkby P.A., Thompson G.H.B. *Opto-Electronics*, **4** (3), 323 (1972).
53. Gasey N.C. Jr., Panise M.B. *Heterostructure Lasers, Part A* (New York: Academic Press, 1978; Moscow: Mir, 1981) Vol. 1.
54. Dolginov L.M., Drakin A.E., Eliseev P.G., Sverdlov B.N., Skripkin V.A., Shevchenko E.G. *Kvantovaya Elektron.*, **11**, 645 (1984); (3), 120 (1971) [*Sov. J. Quantum Electron.*, **14**, 439 (1984); (3), 304 (1971)].
55. Vasil'ev M.G., Dolginov L.M., Drakin A.E., Eliseev P.G., Ivanov A.V., Konyaev V.P., Sverdlov B.N., Skripkin V.A., Shveikin V.I., Shevchenko E.G., Shelyakin A.A., Shepekina G.V. *Kvantovaya Elektron.*, **11**, 631 (1984) [*Sov. J. Quantum Electron.*, **14**, 431 (1984)].
56. Dingle R., Wiegmann W., Henry C.H. *Phys. Rev. Lett.*, **33** (14), 827 (1974).
57. Holonyak N. Jr., Kolbas R.M., Dupuis R.D., Dapkus P.D. *IEEE J. Quantun Electron.*, **16** (2), 170 (1980).
58. Tsang W.T. *Appl. Phys. Lett.*, **39** (10), 786 (1981).
59. Arakawa Y., Sakaki H. *Appl. Phys. Lett.*, **40**, 939 (1982).
60. Drakin A.E., Eliseev P.G. *Kvantovaya Elektron.*, **11**, 178 (1984) [*Sov. J. Quantum Electron.*, **14**, 119 (1984)].
61. Eliseev P.G. *Vvedenie v fiziku inzhektsionnykh lazerov* (Introduction to the Physics of Injection Lasers (Moscow: Nauka, 1963).
62. Zhao X., Komuro S., Isshiki H., Aoyagi Y., Sugano T. *Appl. Phys. Lett.*, **74** (1), 120 (1999).
63. Bresler M.S., Gusev O.B., Terukov E.I., Yassievich I.N., Zakharchenya B.P., Emelyanov V.I., Kamenev B.V., Konstantinova E.A., Timoshenko V.Y. *Techn. Program Photonics West Symp.* (San Jose, CA, 2001) p. 81.
64. Eliseev P.G., Gastev S.V., Koizumi A., Fujiwara Y., Takeda Y. *Kvantovaya Elektron.*, **31**, 962 (2001) [*Quantum Electron.*, **31**, 962 (2001)].
65. Han H.-S., Seo S.-Y., Shin J.H. *Appl. Phys. Lett.*, **79** (27), 4568 (2001).
66. Ekimov A.I., Onushchenko A.A. *JETP Lett.*, **34**, 345 (1981).
67. Efros Al.L., Efros A.L. *Sov. Phys. Semicond.*, **16**, 772 (1982).
68. Ekimov A.I., Onushchenko A.A. *Sov. Phys. Semicond*, **16**, 775 (1982).
69. Eliseev P.G., Karga P.V. *Kvantovaya Elektron.*, **20**, 846 (1993) [*Quantum Electron.*, **23**, 733 (1993)].
70. Cao M., Daste P., Miyamoto Y., Miyake Y., Nogiwa S., Arai S., Furuya K., Suematsu Y. *Electron. Lett.*, **24**, 824 (1988).
71. Kapon E., Tamargo M.C., Hwang D.M. *Appl. Phys. Lett.*, **50**, 347 (1987).
72. Kapon E., Kash K., Clausen E.M. Jr., Hwang D.M., Colas E. *Appl. Phys. Lett.*, **60**, 477 (1992).
73. Saito H., Uwai K., Kobayashi N. *Jpn. J. Appl. Phys.*, **32**, 4440 (1993).
74. Kapon E. *Quantum Wire and Quantum Dot Lasers. Semiconductor Laser I*. Ed. by E. Kapon. (San Diego: Acad. Press, 1999) Ch. 4, pp 291–360.
75. Miyamoto Y., Cao M., Shingai Y., Furuya K., Suematsu Y., Ravikumar K.G., Arai S. *Jpn. J. Appl. Phys.*, **26**, L225 (1984).
76. Hirayama H., Matsunaga K., Asada K., Suematsu Y. *Electron. Lett.*, **30**, 142 (1994).
77. Bimberg D., Grundmann M., Ledentsov N.N. *Quantum Dot Heterostructures* (Chichester: J.Wiley, 1998).
78. Notzel R., Temmio J., Tamamura T. *Nature*, **369**, 131 (1994).
79. Mukai K., Ohtsuka N., Sugawara M., Yamazaki S. *Jpn. J. Appl. Phys.*, **33** (12A), L1710 (1994).
80. Kirstaedter N., Ledentsov N.N., Grundmann M., Bimberg D., Ustinov V.M., Ruvimov S.S., Maximov M.V., Kop'ev P.S., Alferov Zh.I., Richter U., Werner P., Goesele U., Heydenreich J. *Electron. Lett.*, **30** (17), 1416 (1994).
81. Liu G.T., Stintz A., Li H., Malloy K.J., Lester L.F. *Electron. Lett.*, **35** (14), 1163 (1999).
82. Park G., Huffaker D.L., Zou Z., Deppe D.G. *IEEE Photon. Technol. Lett.*, **11**, 301 (1999).
83. Zhukov A.E., Kovsh A.R., Maleev N.A., Mikhrin S.S., Ustinov V.M., Tsatsul'nikov A.F., Maximov M.V., Volovik B.V., Bedarev D.A., Shernyakov Yu.M., Kop'ev P.S., Alferov Zh.I., Ledentsov N.N., Bimberg D. *Appl. Phys. Lett.*, **75** (13), 1926 (1999).
84. Eliseev P.G., Li H., Stintz A., Liu G.T., Newell T.C., Malloy K.J., Lester L. *Appl. Phys. Lett.*, **77** (2), 262 (2000).
85. Zou Z., Huffaker D.L., Gusak S., Deppe D.G. *Appl. Phys. Lett.*, **75** (1), 22 (1999).
86. Wang R.H., Stintz A., Varangis P.M., Newell T.C., Li H., Malloy K.J., Lester L.F. *IEEE Photon. Technol. Lett.*, **13** (8), 767 (2001).
87. Ukhanov A.A., Wang R.H., Rotter T.J., Stintz A., Lester L.F., Eliseev P.G., Malloy K.J. *Appl. Phys. Lett.*, **81** (6), 981 (2002).
88. Basov N.G., Eliseev P.G., Zakharov S.D., Zakharov Yu.P., Oraevsky A.N., Pinsker I.Z., Strakhov V.P. *Fiz. Tverd. Tela*, **8**, 2616 (1966).
89. Eliseev P.G., Sukhov E.G. *Radiotekh. Radioelektron.*, **6**, 1005 (1971).
90. Eliseev P.G., Glebov A.G., Osinski M. *IEEE J. Sel. Topics Quantum Electron.*, **3** (2), 499 (1997).

91. Gill R. *Proc. IRE,* **58** (6), 949 (1970).
92. Murison R.F., Moore A.H., Lee S.R., Holehouse N., Dzurko K.M., Cockerill T.M., Coleman J.J. *Electron. Lett.,* **27** (21), 1979 (1991).
93. Mawst L.J., Bhattacharya A., Botez J., Garbuzov D.Z., DeMarco L., Connoly J.C., Jansen M., Fang F., Nabiev R.F. *Appl. Phys. Lett.,* **69**, 1532 (1996).
94. Zhukov A.E., Kovsh A.R., Mikhrin S.S., Maleev N.A., Odnoblyudov V.A., Ustinov V.M., Shernyakov Yu.M., Kondrat'eva E.Yu., Livshitz D.A., Tarasov I.S., Ledentsov N.N., Kop'ev P.S., Alferov Zh.I., Bimberg D. *Proc. 8th Int. Symp. 'Nanostructures: Physics and Technol.'* (St. Petersburg, 2000) pp 6–11.
95. Kovsh A.R., Zhukov A.E., Maleev N.A., Mikhrin S.S., Vasil'ev A.V., Shernyakov Yu.M., Livshits D.A., Maximov M.V., Sizov D.S., Kryzhanovskaya N.V., Pikhtin N.A., Kapitonov V.A., Tarasov I.S., Ledentsov N.N., Ustinov V.M., Wang J.S., Wei L., Lin G., J.Y. Chi V.A. *Tech. Digest 10th Int.Symp. 'Nanostructure: Physics and Technol.'* (St. Petersburg, 2002) pp 395–398.